EXPERIMENTAL DEVELOPMENT OF KNIFE-PLATE-CONNECTED STEEL PANEL DAMPERS

Po-Chien HSIAO[1], and Chun-Yi LI[2]

SUMMARY

Steel panel dampers (SPDs) have been widely used in the seismic steel building structures usually with brace- or stub-column-type configurations. With the aim of further enlarging ductility capacity and structural efficiency of the SPDs, a novel design, named knife-plate-connected SPD (KSPD), was developed in the study. The proposed KSPD consisted of the steel panel and two side-boundary-columns with pinned end-connections through the knife-plate details as attaching to the beams. The mechanism of the KSPD physically rotates the steel panel of typical SPDs by 90-degree angle in plane, and thereby significantly reduce the aspect ratios of the panel and make its shear deformation similar to the story drift angles. In consequence, the required stiffeners of the panel as well as the required member sizes of the elastic components on the sides of the panel were reduced. Five full-scale KSPD specimens with various stiffener configurations of the panel have been experimentally examined and compared under cyclic loadings. The results verified that the design of KSPDs enabled to achieve significantly high ductility and stable energy dissipation. Increasing the vertical stiffeners effectively postpone the shear buckling of the panel, while the horizontal stiffeners showed minor effect on the shear buckling.

***Keywords**: Steel buildings; Seismic design; Steel panel dampers; Knife-plate connections.*

INTRODUCTION

Steel panel dampers (SPDs) have been widely adopted in the seismic building structures to improve the overall strength and stiffness of the building system for resisting lateral seismic loads. The SPDs typically provide hysteretic energy dissipation to the systems through the shear plasticity of the steel web panel. Prior to the past development of SPDs, the seismic performance of the panel zone at beam-to-column moment resisting connections for the special moment resisting frames (SMRFs) was found to be significantly stable and ductile. Many previous experimental research has confirmed that the steel panel enabled to provide very high ductility and considerable energy dissipation as the design of the weak panel zone was applied, i.e. developing the shear yielding of the web panel (Popov 1987, Krawinkler et al. 1971). The associated modelling approach and design procedures were also developed for the practical use (Kim and Engelhardt 2002, Engelhardt 1999). On the contrary, in the case that the elastic panel zone was excepted in the seismic design, the yielding and buckling of the web panel could be prevented by reinforcing the panel with one or a pair of doubler plates, which was typically adopted in the real practice.

With the feature of the excellent ductility of the steel panel under the seismic loadings, the SPDs were then developed to form one type of metallic damper devices to simultaneously enhance the strength, stiffness and hysteretic damping of the structural systems. To advance the seismic performance of SPDs, many previous studies have investigated the SPDs through either experimental and analytical approaches (Matteis et al. 2003, Tsai et al. 2018, Hsiao and Liao 2019). With the aim of enlarging the deformation capability of SPDs, the low-yield steel

[1] *Associate Professor, National Taiwan University of Science and Technology, Taiwan, e-mail: pchsiao@mail.ntust.edu.tw*
[2] *Graduate student, National Taiwan University of Science and Technology, Taiwan*

was adopted for the inelastic panel segments of the SPDs. Many experimentally and analytically investigations of this type of SPDs were conducted (Nakashima 1995, Zhao et al. 2022). Their results confirmed that the low-yield SPDs typically had severe strength hardening effect which required to be considered in the design of surrounding frame systems. To postpone the shear buckling of the steel panels, various restraining strategies were proposed including to adopt corrugated steel panel (Xu et al. 2016), to add panel stiffeners (Wang et al. 2021, Chen et al. 2006) and even to use buckling restrained components (Tamai 2015). Their results confirmed that the aspect ratios and plate thickness of the web panels were the major design parameters governing the hysteretic performance of the SPDs.

The typical SPD consists of the inelastic panel and the elastic connecting segments. While the inelastic panel segment was designed to form a shear plastic hinge and provide the energy dissipation, the elastic connecting segments with various configurations were adopted to connect the steel panel to the surrounding frame systems. Among the real building applications, the SPDs have been commonly installed in frame systems using brace-type and stub-column-type configurations, as illustrated in Figs. 1(a) and 1(b), respectively. The brace-type configuration allows to form a greater overall stiffness, but enlarges the deformation demand at the SPD and limits the architectural versatility in the span. On the contrary, the SPD with the stub-column-type configuration permits improved architectural versatility in the span and deformation capacity due to the greater height of SPDs in the story, but usually results in smaller increases of the system stiffness compared to the brace-type ones. Either the brace- or stub-column types, the elastic connecting segments of SPDs were typically required to be sufficiently strong and stiff by using much greater member sizes compared to the inelastic panel one to ensure their elasticity under the associated extreme loads of the inelastic panel and to achieve relatively great stiffness of the members.

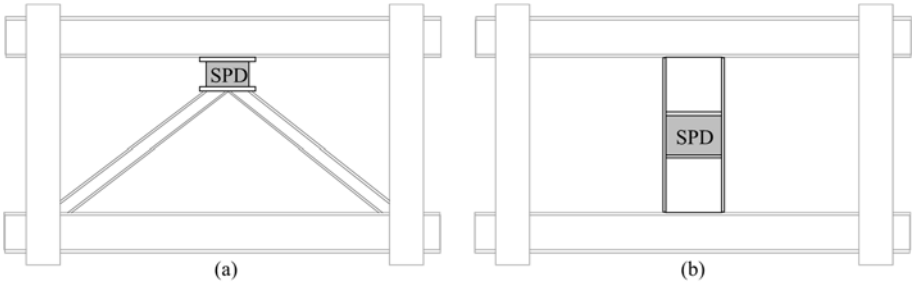

Figure 1. Applications of SPDs with (a) brace-type, and (b) stub-column-type configurations.

The study here proposed a novel design of the stub-column-type SPD devices, named as knife-plate-connected SPDs (KSPDs), with the aim of improving the structural efficiency of the SPDs as well as mitigating the deformation amplification of the steel panel of SPDs. In terms of the structure of the KSPD, the steel panel was first attached to two boundary columns on the sides, which connect to the surrounding beams through knife-plate connections at top and bottom ends, as illustrated in Fig. 2. The basic mechanism of the developed KSPD is first described in the study. An experimental program, containing a serious of full-scale KSPD specimens subject to cyclic loading including fatigue testing, is then presented to evaluate the seismic performance of the KSPDs. The yielding, buckling and failure behaviors of the KPSD were evaluated, and the effects of the panel stiffeners and the seismic performance of the knife-plate connections were investigated upon the experimental results.

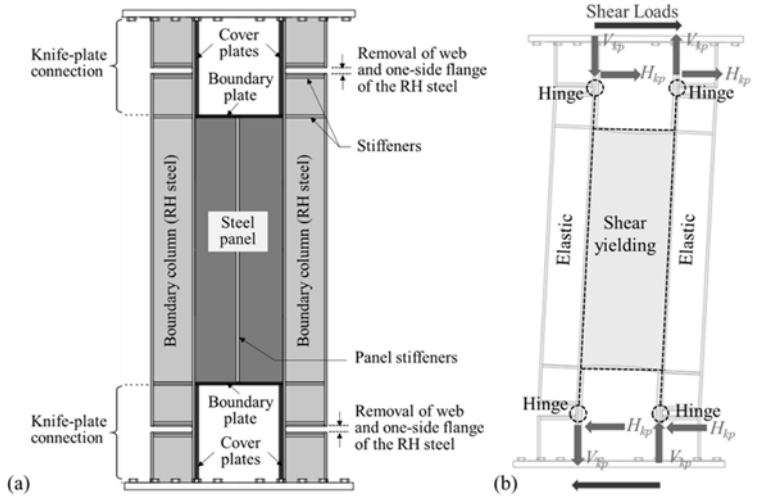

Figure 2. The scheme of (a) the structure, and (b) the deformed shape of the KSPD.

DESIGN MECHANISM OF THE KSPD

The current existing SPD consists of the middle inelastic panel and the elastic connecting segments, which were typically arranged vertically in the installed span, as shown in Fig. 1. Due to that the lateral deformations were majorly concentrated at the inelastic panel through shear yielding under the applied lateral loads, much higher deformation demands compared to the associated story drifts were happened at the inelastic panels. To prevent the high deformation demands of the inelastic panel, the proposed KSPD changed the arrangement of the middle inelastic panel and elastic connecting segments to a horizontal manner. The middle steel panel was attached to two boundary columns of rolled H-section (RH) steel connected to the surrounding beams of the framing systems through end knife-plate connections, as illustrated in Fig. 2(a). The details of the knife-plate connections were designed to form a hinge-like behavior, i.e. providing negligible moments, while maintaining a relatively low cost, and thereby released the end moments of the columns, as shown in Fig. 2(b). An one-t_{kp}-linear clearance of the knife plate was formed by removing the column web and one-side flange of the RH steel as shown in Fig. 2(a), where t_{kp} is the thickness of the knife plate. It should be noted that the knife plate should be designed to be capable of transferring both the shear and axial forces, i.e. H_{kp} and V_{kp} respectively as illustrated in Fig. 2(b), at the clearance band of the knife plate. With the mentioned large force demands of the knife plates, cover plates might be additionally welded to the column flanges around the clearance to provide sufficient strengths. This configuration of the KSPD with low aspect ratios only permitted the steel panel to develop shear yielding and the lateral resistance, as shown in Fig. 2(b), while the shear deformations of the panel spread out over the entire height of the panel similar with the story drifts in the given story. All edges of the steel panel were reinforced by the boundary columns and boundary plates, as shown with dashed-lines in Fig. 2(a). In addition, several panel stiffeners could be added to the steel panel if needed through welding to further postpone or even prevent shear buckling of the steel panel, and thereby enlarge the member ductility. The abovementioned design of the KSPD created a simple mechanism of shear behavior of the steel panel as well as a simplified structure of the member, which therefore benefited the simplicities of the design method and the modelling approaches.

EXPERIMENTAL PROGRAM OF KSPDS

A series of full-scale KSPD specimens were tested in the study to experimentally examine and verify the feasibility and the seismic performance of KSPDs, and also clarify the effect of the configurations of panel stiffeners on the buckling prevention. To simulate the boundary conditions of KSPD in the frame systems, a four-hinges loading frame system, as shown in Fig. 3(a), was adopted to form a double-curvature mechanism of the specimens. A 2225kN hydraulic actuator was adopted horizontally at the top of the loading frame to provide lateral loads. The top beam of the loading frame was an approximately fixed-end boundary condition to the upper end of the specimen, as the bottom end of the specimen was anchored to the floor beam forming an exact fixed-end boundary condition. The four-hinges loading frame provided no lateral resistance, and the top beam was designed to remain straight and horizontal during the loading. A lateral support system was used to prevent the top beam against out-of-plane displacements by a pair of angles (L 200×200×20).

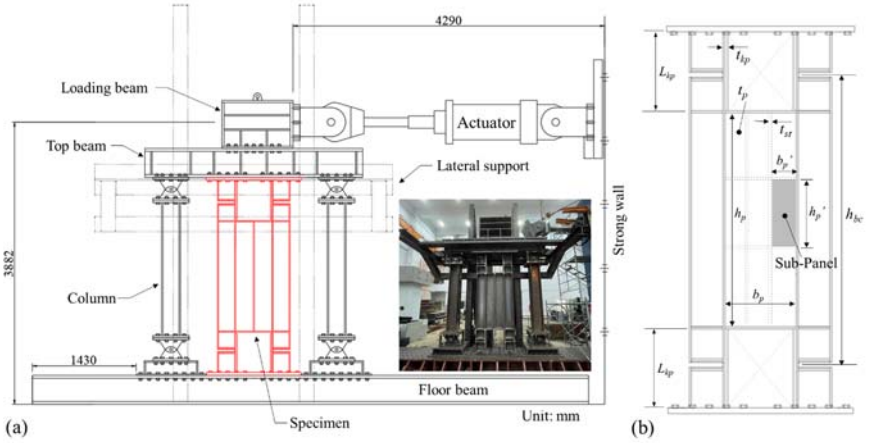

Figure 3. Adopted test setup of the experimental program.

The specimens with a net height of 2720mm were installed between the floor beam and the top beam as shown. No axial load, i.e. external gravity load, of the members was applied in the study, i.e. the effect of the axial loads

on the seismic performance of the KSPD was neglected in the study. The required loading protocol for beam-to-column moment connection in the SMRF specified in AISC 341-16 was adopted in the study. Additionally, four elastic cycles of 0.125% story drift were added at the beginning of the loading protocol considering the shear yielding of steel panel might be earlier, and two cycles at 5.0% story drift level were additionally added at the end of the protocol to examine the ductility capacity of KSPDs, as illustrated in Fig. 4. The resulting increasing amplitude cyclic loading protocol is referred to the standard cycles hereinafter. Fatigue cycles of 4.0% story drift were continuously performed until meeting the specimen failure, defined as the remaining strength dropped to 80% of the maximum strength, after the standard cycles described above.

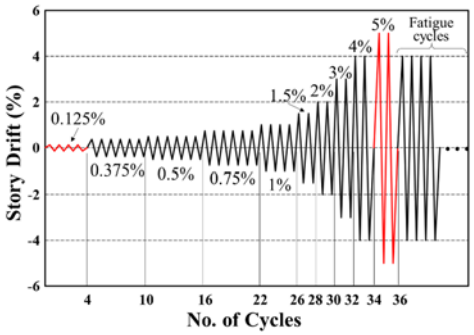

Figure 4. Adopted cyclic loading protocol.

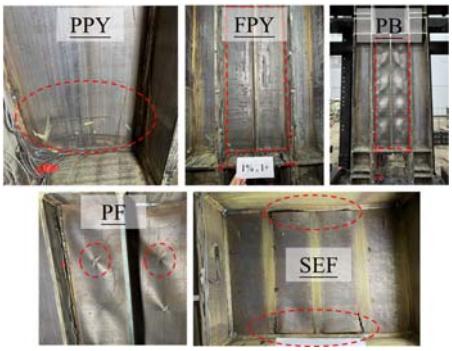

Figure 5. Various yield mechanisms and failure modes of the steel panels.

Design of specimens

With the aim of verifying the seismic performance and the effect of panel stiffeners of KSPDs, five full-scale KSPD specimens were experimentally tested in the study. Those specimens generally shared identical dimensions of the steel panel, boundary columns and the details of knife-plate connections. The rolled H-section of RH250×255×14×14 was consistently adopted for the boundary columns of the steel plates having the width (b_p) of 500mm, the height (h_p) of 1500mm and the thickness (t_p) of 6mm, as shown in Table 1 and Fig. 3(b). All specimens were fabricated with SN400YB steel grade, including the steel panel, boundary elements, stiffeners, cover plates, etc..

The knife-plate connections, as shown in Fig. 2, consistently had a length (L_{kp}) of 570mm. The knife plates were formed by removing the web and one-side flange of the RH within a linear clearance of 34mm, which was approximately in the middle of the connections. Cover plates of 20mm were welded to the remaining flange (14mm thick) within the entire length of the knife-plate connections to form an overall thickness of knife plate (t_{kp}) by 34mm. It made the consistent distance between the centers of two linear clearances of the knife plates (h_{bc}) 2000mm, as shown in Fig. 3(b). The lateral yield strength of the KSPD, V_y, mainly governed by the shear yielding of the middle steel panel, could be estimated by Eq. (1) upon the equilibrium of the free-body diagram shown with dashed lines illustrated in Fig. 2(b).

$$V_y = \frac{0.6F_{y,p}h_p t_p b_p}{h_{bc}} = 0.6F_{y,p}t_p b_p R_h \tag{1}$$

Where $F_{y,p}$ is the yield strength of the steel panel. R_h is the height ratio of h_p to h_{bc}. H_{kp} and V_{kp} in the figure are horizontal (longitudinal) and vertical (transverse) loads developed at each knife plate under lateral loads applied, respectively, with the relation of Eq. (2), as the moment resistance of the knife plate is neglected.

$$H_{kp}h_{bc} = V_{kp}b_p \tag{2}$$

The Eq. (1) was according to the situation as the V_{kp} and H_{kp} of Eq. (2) equal to $V_y/2$ and $0.3F_{y,p}t_p h_p$, respectively. The specimens in the study were basically named by the arrangement of the panel stiffeners, where a title of "SV" followed by the number of the vertical stiffeners (#), i.e. SV1, SV2, etc., was used. If both the horizontal stiffeners were also included in the specimens, a title of "H" followed by the number of the horizontal stiffeners was added after the name of "SV#." For instance, Specimen SV1H2 contained one vertical and two horizontal stiffeners of the panel. The 15mm thick stiffeners (t_{st}) with the width of 125mm (b_{st}) were consistently used in the study including that on the boundary columns and knife-plate connections as shown in the figure. It should be noted that the vertical and horizontal stiffeners were attached at two different sides of the panel with equal intervals to form

the sub-panels with the width (b_p') and height (h_p'), as shown in Fig. 3(b) and Table 1. N_{vst} and N_{hst} listed in the table are the numbers of the panel stiffeners oriented vertically and horizontally, respectively. Among the specimens shown above, five different configurations of panel stiffeners with various b_p' and h_p' were experimentally compared to evaluate the influence on their seismic performance, especially the buckling behavior of the panels. The yield and tensile strengths of each element of the specimen based on the tensile tests are summarized in Table 2.

Table 1. Detailed dimensions of the KSPD specimens

Specimens	Boundary Beams / Knife-Plate Connections				Steel Panel					Panel Stiffeners			
	Section (mm)	L_{kp} (mm)	t_{kp} (mm)	h_{bc} (mm)	h_p (mm)	b_p (mm)	h_p' (mm)	b_p' (mm)	t_p (mm)	t_{st} (mm)	b_{st} (mm)	N_{vst}	N_{hst}
SV1	RH 250×255×14×14 (SN400YB)	570	34	2000	1500	500	1500	250	6	15	125	1	-
SV2							1500	167				2	-
SV3							1500	125				3	-
SV1H2							500	250				1	2
SV3H3							375	125				3	3

Table 2. Material properties of each element of the KSPD specimens upon tensile tests

Elements	Steel Grade	Thickness (mm)	Yield strength F_y (MPa)	Tensile strength F_u (MPa)
Steel panels	SN400YB	6	283	404
Stiffeners / Boundary plates		15	341	512
Cover plates		20	293	433
Flanges of boundary columns		14	299	418
Webs of boundary columns		14	301	442

Test results and observations

A series of pilot experiments with five KSPD specimens with various configurations of panel stiffeners were conducted using the cyclic loading protocol mentioned above. All specimens generally performed high ductility and stable hysteretic behavior as described follows, which experimentally verified the seismic mechanism and the feasibility of the KSPDs developed in the study. The steel panel in general would first develop shear yielding. The buckling of the panel would possibly occur afterward, and finally led to various types of panel fracture. The observed yield mechanisms and failure modes included partial panel yielding (PPY), full panel yielding (FPY), panel buckling (PB), panel fracture (PF), and sub-panel-edge fracture (SEP), as shown in Fig. 5. As the knife-plate connections were aimed to form a hinge-like behavior as mentioned above, the observed yield mechanisms and failure modes throughout specimens included knife-plate initial yielding (KIY), knife-plate severe yielding (KSY), knife-plate fracture initiation (KFI), and knife-plate severe fracture (KSF), as shown in Fig. 6. In general, the yield mechanism was approximately triggered by 0.5% story drift, while the buckling or fracture behavior occurred beyond the cycles of 4.0% story drift in the study.

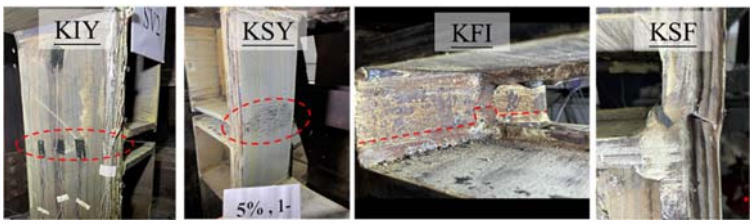

Figure 6. Various yield mechanisms and failure modes of the steel panels.

The measured hysteretic responses of the five specimens under the standard cycles were shown in Figs. 7(a)-(e), respectively. The observations of all mentioned mechanisms and failure modes above are marked in the figures. The yield strength, V_y, calculated upon Eq. (1) using the measured yield strength obtained from the tensile tests, and $1.5V_y$, representing the ultimate strength, are referenced in the figures. The results verified that the PPY consistently occurred in the cycles of 0.5% story drifts among specimens, while the FPY consistently occurred in the cycles of 1.0% story drifts throughout specimens. In terms of knife-plate connections, the KIY was consistently initiated in the cycles of 1.0% story drifts. The yielding would term obvious, as represented by the KSY, until the cycles of 5.0% story drifts. It should be noted that the PB behavior was only observed in SV1 and SV1H2

specimens, having the fewest vertical stiffeners, in the cycles of 4.0% story drifts, as shown in Figs. 7(a) and 7(d), respectively. The PB would result in apparent pinching of hysteretic loops and therefore reduction of overall strengths and energy dissipation. Without the PB behavior, the rest of specimens, i.e. SV2, SV3 and SV1H3, could experience full hysteretic loops, followed by greater ultimate strengths and the KFI in the cycles of 5.0% story drifts as shown in Figs. 7(b), 7(c) and 7(e), respectively.

All specimens of the study had finished the standard cycles without apparent failure, and the tests were continued for the fatigue cycles to examine the cumulative ductility of the specimens. The measured hysteretic results of the fatigue tests are shown in Figs. 8(a)-(e). The results verified that specimens with various arrangement of panel stiffeners would have various ultimate failure modes, including the PF, KFI and SEF, and cumulative ductility of specimens. Among specimens, the SV1 and SV1H2 specimens (Figs. 8(a) and 8(d)), which experienced panel buckling in the standard cycles, continued the pinching hysteretic behavior in the fatigue cycles, and sustained six and two fatigue cycles, respectively, until the end of tests when the PF along with KFI were observed. Specimen SV2 (Fig. 8(b)), having no PB observed in the standard cycles, started developing PB after ten fatigue cycles, and the test was terminated due to the failure modes of PF and KSF observed at the 13th cycles of the fatigue. With more vertical panel stiffeners, the PB of the SV3 was further postponed, as shown in Fig. 8(c). The test was terminated until the KSF observed after 20 fatigue cycles. Slight PB could be observed at the end of the test, as no pinching of the hysteretic loops was shown. It should be noted that the KSF, as shown in Fig. 6, would not result in apparent strength degradation of the specimen, instead, the strength of the specimen gradually decreased with stable and considerable energy dissipation. Similar to SV3, Specimen SV3H3 had no significant PB and pinching behavior until the end of the test, as shown in Fig. 8(e). However, the PB and KSF were observed earlier around the tenth fatigue cycle, which were considered due to the existing of horizontal panel stiffeners and greater ultimate strength of the specimen respectively. Moreover, the failure mode of SEF was also observed beyond the tenth fatigue cycle, and led to relatively obvious strength degradation, as shown in Fig. 8(e). The test was terminated after 15 fatigue cycles as the strength dropped to 80% of its maximum strength. The results verified that the installation of the horizontal panel stiffeners, such as SV1H2 and SV3H3, would actually reduce the cumulative ductility, i.e. fatigue life, of the specimens as compared to SV1 and SV3, respectively.

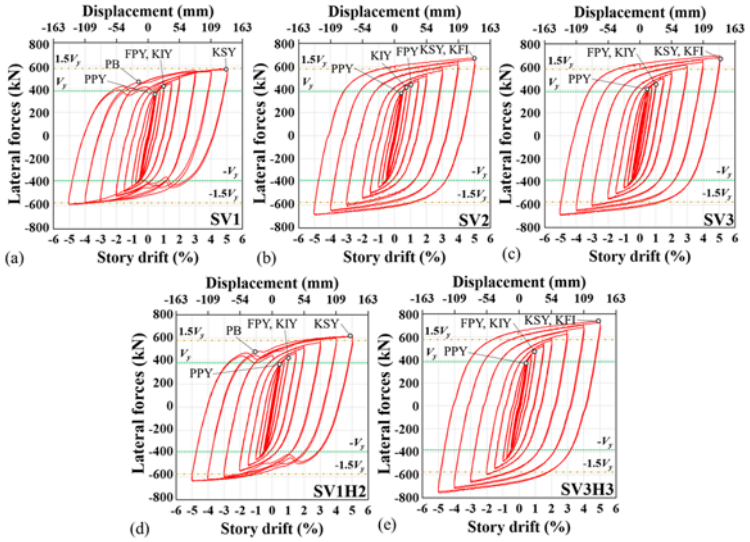

Figure 7. Measured hysteretic behaviors of specimen (a) SV1, (b) SV2, (c) SV3, (d) SV1H2 and (e) SV3H3.

Strength backbones and the ductility of specimens

The strength backbone curves of all specimens were summarized and compared in Fig. 9(a). It verified that five specimens had very similar elastic stiffness and yield strengths even though they had various panel-stiffener configurations. The major yielding of specimens consistently occurred around the story drift of 0.5% radians, as the yield strengths, V_y, could be approximately estimated by Eq. (1). The results confirmed that the yield mechanism of the KSPD was mainly governed by the shear yielding of the steel panel, as the rest portions of specimens remained elastic. However, beyond the yield strengths, all specimens presented various post-yield tangent stiffness as shown. Among specimens, SV1 and SV1H2 specimens presented relatively lower post-yield stiffness and a minor drop of the tangent stiffness beyond 4% story drift where panel buckling occurred in the tests. It led to the ultimate strengths of specimen approximately were about $1.5V_y$. With no panel buckling occurred, the

other specimens developed relatively higher post-yield strengths and stiffness. It was apparent that the post-yield strengths would increase with the adopted number of panel stiffeners including vertical and horizontal ones. It showed that the panel stiffeners would slightly contribute the overall strengths of the member. To precisely consider the effect of the panel stiffeners on the strength capacity, a strength hardening ratio (ω) of 1.65 may be conservatively used.

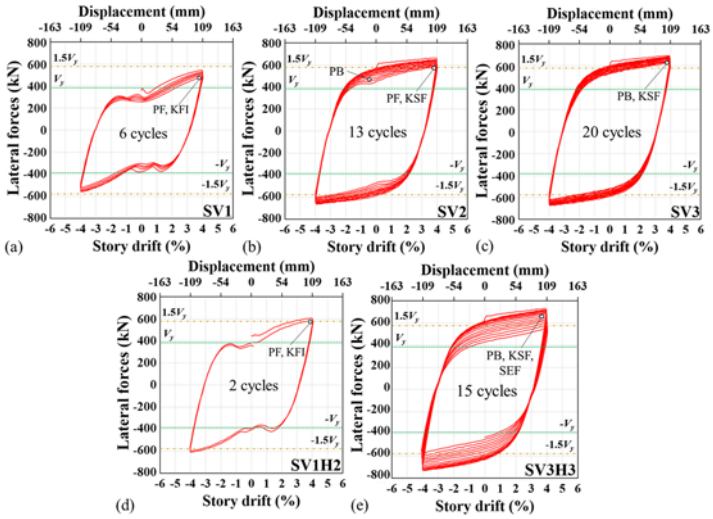

Figure 8. Measured fatigue behaviors of specimen (a) SV1, (b) SV2, (c) SV3, (d) SV1H2 and (e) SV3H3.

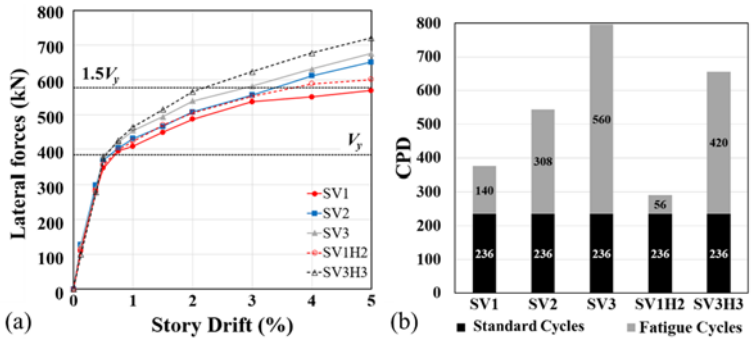

Figure 9. Comparisons of (a) strength backbone curves, and (b) the cumulative plastic deformations (CPD) of specimens.

All specimens in the study completed the standard cycles without apparent failure. It verified that with proper arrangement of panel stiffeners, the proposed KSPD would potentially have significant ductility capacity at least up to 5% story drift level as well as the cumulative ductility. Figure 9(b) showed the measured cumulative plastic deformations (CPD) of specimens including both of the standard and fatigue cycles in the tests. It shows that all specimen accumulated similar CPD values, about 236, in the standard cycles and varied significantly in the fatigue cycles. Comparing the results of specimens SV1 to SV3, it was verified that increasing the vertical panel stiffeners would apparently enlarge the CPD of the member. The maximum CPD of the specimen reached the value of 800 (SV3), which was 211% increase compared to the SV1 specimen. By comparing the SV1 and SV3 with SV1H2 and SV3H3, respectively, it showed that adding the horizontal stiffeners actually reduced the overall CPD values by 22% and 18% for the SV1H2 and SV3H3 cases, respectively.

CONCLUSIONS

A novel design of KSPD has been developed by changing the typical vertical arrangement of the middle inelastic panel and elastic connecting segments to a horizontal manner. The details of knife-plate connections with the 1tkp-clearance rule have been developed to connect the elastic connecting segments, i.e. boundary columns, to the surrounding beams of the frame system with the feature of moment releasing. The configuration of the proposed KSPD would prevent the deformation amplification at the steel panel and therefore created a simpler and economical shear-yielding damper device. The seismic performance of the KSPD including five full-scale specimens were experimentally evaluated in the study.

REFERENCES

Popov, E.P. (1987) “Panel zone flexibility in seismic moment joints,” *Journal of Constructional Steel Research*, **8**, pp.91-118.

Krawinkler, H., Bertero, V.V., Popov, E.P. (1971) “Inelastic Behaviour of Steel Beam-to-Column Subassemblages,” *Report No. **EERC-71/7** Earthquake Engineering Research Center*, University of California.

Kim, K.D., Engelhardt, M.D. (2002) “Monotonic and cyclic loading models for panel zones in steel moment frames,” *Journal of Construction Steel Research*, **58** (5), pp. 605-635.

Englekirk, P.E. (1999) “Extant panel zone design procedures for steel frames are questioned,” *Earthquake Spectra*, **15**(2), EERI, Oakland, California, USA.

Matteis, G.D., Landolfo, R., Mazzolani, F.M. (2003) “Seismic response of MR steel frames with low-yield steel shear panels,” *Engineering Structures*, **25**(2), pp.155-168.

Tsai, K.C., Hsu, C.H., Li, C.H., Chin, P.Y. (2018) “Experimental and analytical investigations of steel panel dampers for seismic applications in steel moment frames,” *Earthquake Engineering & Structural Dynamics*, **47**(6), pp.1416-1439.

Hsiao, P.C., Liao, W.C. (2019) “Effects of Hysteretic Properties of Stud-type Dampers on Seismic Performance of Steel Moment Resisting Frame Buildings,” *Journal of Structural Engineering*, ASCE, **145**(7): 04019065.

Nakashima, M. (1995) “Strain-hardening behavior of shear panels made of low-yield steel. I: test,” *Journal of Structural Engineering*, **121**(12), pp.1742-1749.

Zhao, J. Z., Tao, M. X., Wu, Z. H., Zhuang, L. D. (2022) “Experimental and numerical study on bent shear panel damper made of BLY160 steel,” *Engineering Structures*, **260**, 114229.

Xu, L.Y., Nie, X., Fan, J.S. (2016) “Cyclic behaviour of low-yield-point steel shear panel dampers,” *Engineering Structures*, **126**, pp.391-404.

Wang, W., Song, J., Su, S., Cai, H., Zhang, R. (2021) “Experimental and numerical studies of an axial tension-compression corrugated steel plate damper,” *Thin-Walled Structures*, **163**, 107498.

Chen, Z., Ge, H., Usami, T. (2006) “Hysteretic model of stiffened shear panel dampers,” *Journal of Structural Engineering*, **132**(3), pp.478-483.

Tamai, H. (2015) “On Equivalent Shear Buckling Deformation Angle for Shear Panel Damper, ” *Journal of Structural and Construction Engineering*, AIJ, **87**(707), pp.137-145. (in Japanese)